THE COOLING EFFECT OF BEAM SELF-FIELDS ON THE PHOTOCATHODE SURFACE IN HIGH GRADIENT RF INJECTORS

Y. Chen*, M. Krasilnikov, F. Stephan, Deutsches Elektronen-Synchrotron, 15738 Zeuthen, Germany

Abstract

The intrinsic slice emittance of the emitted electrons on the photocathode surface at each moment during the transient photoemission process depends on the transverse size of the slice and the mean kinetic energy of the electrons within the slice. The latter relies on the surface barrier potentials of the cathode material at a fixed wavelength of the incident light, and is thus significantly influenced by the presence of strong rf and beam self-fields at / close to the cathode surface. This is, in particular, the case in high brightness injectors for modern free electron lasers. In this article, the beam self-fields are determined in a self-consistent approach, based on which improved transverse and temporal emission distributions are obtained. The nonlinear correlations of the intrinsic surface slice emittance within the bunch are shown for multiple bunch charges. A peak to peak variation of the intrinsic surface emittance is estimated as 30% for the highest charge-density case considered in this paper. An overall reduction of the average intrinsic emittance is computed as 10% accordingly. The cooling effect on the cathode surface is enhanced as the local space-charge density rises. The impacts of the cooling effect on downstream beam qualities are demonstrated through particle tracking simulations based on the injector setup at the Photo Injector Test Facility at DESY in Zeuthen (PITZ).

INTRODUCTION

High brightness electron sources are widely applied in modern free electron lasers (e.g. European XFEL [1] and FLASH [2]) for providing short electron bunches (typically a few to a few tens of picoseconds) of high bunch charge (~nC), very small transverse normalized emittance (<1 mm mrad) and small energy spread (<1%). Semiconductor photocathodes (e.g. Cs_2Te) are prevalently used in such electron sources. The intrinsic beam emittance originated from the photocathode, as a lower limit of the optimized transverse emittance, is becoming increasingly important [3, 4]. The overall shape of the slice emittance curve, for instance, contains a large fraction of the intrinsic beam emittance. The latter can only be determined through proper modeling of the photoemission process in the presence of (strong) collective effects in the gun. For extracting desirable high-charge (density) electron bunches of required transverse emittance, the operation conditions of high gradient rf guns often lead to an emission regime at beam extraction, namely, space-charge dominated photoemission [5,6], where strong space-charge effects influence the emission process through complex interplay in the cathode vicinity. In this article, we consider the impact of beam self-fields onto the formation

_____
* ye.lining.chen@desy.de

of slice emittance at extraction by introducing transverse phase-space nonlinearities and nonlinear correlations along the bunch.

ELECTRON EMISSION MODELING

To account for beam self-fields in the transient process of photoemission (PE), an enhanced PE model is applied. The quantum efficiency (QE) formalism for semiconductors [7, 8] reads

$$QE = \eta \frac{8}{\Lambda^4} \int_1^\Lambda \zeta^3 f(\zeta) d\zeta \qquad (1)$$

with

$$f(\zeta) = \frac{(1-\zeta)(2\zeta p - \zeta - 1)}{2\zeta^2} + p^2 \ln\left[\zeta\left(\frac{1+p}{1+\zeta p}\right)\right] \quad (2)$$

The scattering fraction function, $f(\zeta)$, characterizes the scattering effect during PE accounting for the probability for an electron to survive from successive collisions on its path to the cathode surface. The symbol ζ refers to the cosine of a defined polar angle with respect to the normal to the cathode surface. The term Λ is defined as the square root of the ratio between ΔE and the electron affinity E_a with $\Delta E = \hbar\omega - E_g$, that is, the energy difference between the incident photon energy ($\hbar\omega$) and the band gap (E_g) of the cathode material. The variable p physically interprets the ratio of the drive laser penetration depth (δ) to the average distance (l) an electron travels between collision events, i.e., $p = \delta/l$. The average distance can be computed as $\tau(2m\Delta E)^{0.5}/m$, where the effective mass $m = (E_g/R_\infty)m_0$ with R_∞, m_0 and τ denoting Rydberg energy, electron rest mass and the scattering time, respectively. In principle, smaller p results in larger f, i.e. a larger fraction of surviving electrons from the scattering process. Given the laser penetration depth at a certain wavelength, the decrease of p corresponds to the increase of the effective distance between collision events leading to a higher probability of the electrons being transported to the cathode surface. Additionally, the term η is proportional to the reflectivity coefficient (R) of the cathode which depends on the drive laser wavelength [9]. The calculation of the scattering time is based on [7] and will not be discussed in detail. For near-threshold PE, the cathode QE can be further reduced to

$$QE\left[\Phi_{\text{eff}}(r_\perp, t)\right] = \frac{\alpha}{\left[1 + E_a/\Phi_{\text{eff}}(r_\perp, t)\right]^2}, \qquad (3)$$

where the form factor $\alpha = \eta/(1+p)$ with p described in Eq. (2) and the term Φ_{eff} represents the effective cathode work function for describing the probability of electron escape from the cathode surface by overcoming the surface barrier potentials, $\Phi_{\text{eff}} = \Phi_0 \pm \Phi_{\text{schottky}}$. The terms

MC5: Beam Dynamics and EM Fields

D08 High Intensity in Linear Accelerators - Space Charge, Halos

Φ_0 and $\Phi_{schottky}$ refer to the intrinsic cathode work function and the modifications of Φ_0 due to the Schottky-like effect, respectively. The latter can be expressed as $\Phi_{schottky} = e\sqrt{e[E_{rf}(r_\perp, t, z = 0) + E_{sc}(r_\perp, t, z = 0)]/4\pi\epsilon_0}$ with e and ϵ_0 denoting electron charge and vacuum permittivity, respectively. The symbols E_{rf} and E_{sc} stand for the spatial and temporal dependent parameters: the rf and beam self-fields at the cathode position, respectively. The symbol "$\pm$" in Φ_{eff} marks the moment when the full field changes its sign at $z = 0$ which refers to the cathode surface position. The symbols $r_\perp$ and t represent the spatial and temporal dependencies of the cathode QE. Based on Eq. (3), the transient charge production can be expressed as

$$dQ(r_\perp, t) = \frac{e\alpha dE_{las}(r_\perp, t)dr_\perp dt}{\hbar\omega\left[1 + E_a/\Phi_{eff}(r_\perp, t)\right]^2}, \quad (4)$$

where dE_{las} represents energy of the cathode drive laser pulse. The extracted total charge is then computed as the integration of Eq. (4) over the laser-illuminated area on the cathode surface during emission.

INCORPORATION OF PE MODEL WITH NUMERICAL APPROACH

Due to the fact that the beam self-fields are not prior known, a proposed space-charge iteration approach in [5] is applied in this paper to incorporate with Eqs. (3) and (4) in order to compute, in a self-consistent manner, the contribution of the beam self-fields onto the cathode QE during the transient emission process, and thus the numerically converged temporal profile of the emitted bunch through particle tracking simulations. Note that the locally produced charge in this approach strongly depends on the spatial ($\perp$) and temporal (t) dependent local fields. Interested readers are referred to [5] for a detailed description of the algorithm.

CATHODE DRIVE LASER DIAGNOSTICS

To provide an initial electron distribution generated at the cathode for the space-charge iteration approach, the cathode drive laser pulse needs to be more accurately characterized. Mature diagnostic techniques at PITZ are employed for determining the transverse and longitudinal laser distributions by using the virtual cathode method (see [10] for descriptions) and the optical sampling system (OSS, see [11] for descriptions), respectively. Figure 1 shows the measured transverse laser spot of about 0.8 mm in diameter and the measured quasi flattop-shaped temporal laser profile of about 7.4 ps in FWHM.

COOLING EFFECT OF BEAM SELF-FIELDS ON CATHODE SURFACE

Through particle tracking simulations, the transient emission process is resolved according to Eqs. (3) and (4) based on the space-charge iteration approach. Key simulation parameters are summarized in Table 1. Computation of the intrinsic emittance follows theoretical derivations in [12],
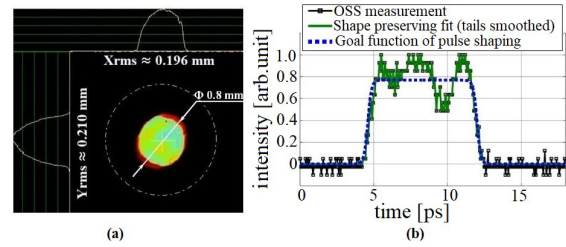

Figure 1: Experimentally determined cathode drive laser transverse (a) and temporal (b) distributions.

which clarifies that the intrinsic emittance depends on the rms beam size and the square root of the rms of the dimensionless transverse momentum. As discussed earlier, the effective cathode work function is time- and space-dependent according to the spatial and temporal dependent fields formulated in the cathode QE during the transient emission process. This leads to a correlation of the sliced intrinsic surface emittance with the emission time clock.

Table 1: Simulation Parameters

Max.field gradient	57.2	MV/m
RF gun phase	0[1]	degree
Laser spot diameter	0.8	mm
Laser pulse length	7.4[2]	ps
Laser distributions	Fig.1[3]	n/a
Laser wavelength	257	nm
Cathode type	Cs_2Te	n/a

[1] with respect to the maximum mean momentum gain phase

[2] full width at half maximum

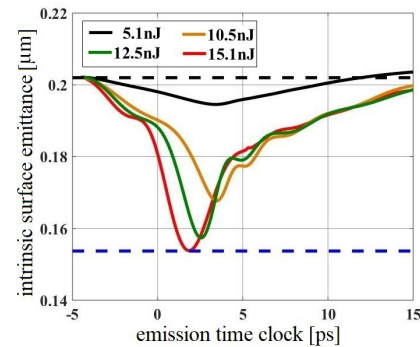[3] green curve in Fig.1(b) used as the temporal laser distribution

Figure 2: Transient intrinsic surface emittance. Dashed lines mark the peak to peak variation of the emittance.

Figure 2 shows the intrinsic beam emittance on the cathode surface as a function of the emission time clock for different incident energies of the cathode drive laser pulse. As shown, illuminated with a fixed laser wavelength, the surface of the Cs_2Te photocathode is prominently cooled down. With growing energies of the laser pulse striking the cathode, more photo-emitted electrons are produced on the cathode surface resulting in a rising local space-charge density,
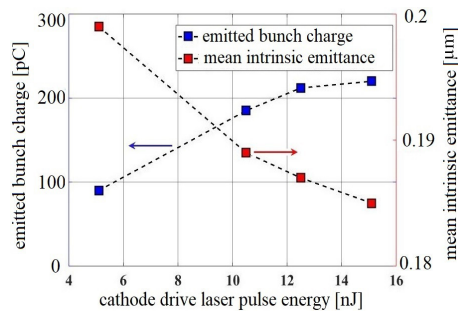
Figure 3: Characteristic emission curve (left axis) and the simulated mean intrinsic surface emittance (right axis).

Figure 4: Simulated slice emittance at EMSY1.
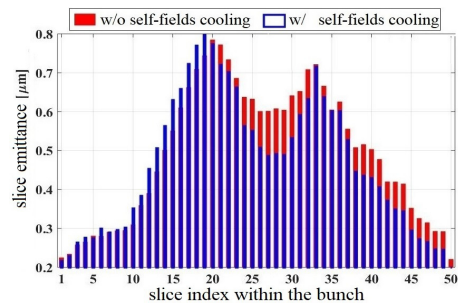
and thereby a growing beam self-field. This increases the effective cathode work function and lowers the kinetic energy of the photo-electrons which can be further extracted from the cathode surface. A lower intrinsic surface emittance is thus resulted for a given laser spot size. In this case, it shows a peak to peak variation of the intrinsic surface emittance by 30%. Moreover, the cooling effect changes the correlation of the sliced intrinsic emittance with time and introduces nonlinearities to the formation of the beam phase space at extraction. As shown in Fig. 2, the transient evolution of the slice emittance follows the development of the space-charge density on the cathode surface. At first moments of emission, the intrinsic emittance tends to grow due to the applied rf field reducing the cathode effective work function when the space-charge density is still low. As the space-charge density is built up on the cathode surface, the fast growing beam self-field counteracts the rf field causing a relative increase in the surface potential barrier and rendering a lower intrinsic surface emittance. The deep valleys appearing close to the middle of the emission process correspond to the highest space-charge density in individual cases, i.e. the strongest cooling periods during emission. For higher space-charge densities, the onset of the valley is shifted to earlier time clock. As the emitted electrons accelerated by the rf field thereby leaving the cathode vicinity, the beam self-field on the cathode surface is weakened. As a result, the cathode work function is decreased accordingly. A gradual increase of the kinetic beam energy, i.e. the intrinsic emittance, is then shown toward the end of the emission process, meanwhile, the rf field on the cathode surface is becoming dominant.

Figure 3 shows the total emitted bunch charge versus the energy of the cathode drive laser pulse (left axis) and the simulated mean intrinsic surface emittance accordingly (right axis). As shown, the cooling effect of the beam self-fields on the cathode surface tends to be more prominent as the charge extraction approaches to the space-charge dominated emission regime (nonlinear part of the curve shown on the left axis). The cooling strength in terms of the mean intrinsic emittance (for the simulation results shown in Fig. 2) is about 10% along the emission curve.

DOWNSTREAM SLICE EMITTANCE

Furthermore, the impact of the beam self-fields induced cooling effect on downstream slice emittance is explored by simulations. The simulation setup is based on the standard injector setup at PITZ [4]. Figure 4 illustrates the computed slice emittance at the position of the first emittance measurement station (EMSY1, z ≈ 5.27 m downstream the cathode) for the 15.1 nJ case as shown in Fig. 2. The horizontal axis is in correspondence with the time clock varying from left (bunch head) to right (bunch tail). The comparison of the sliced beam emittance between with (blue bars) and without (red bars) implementation of the cooling effect has demonstrated, that the tail part of the bunch has lower slice emittance compared to the head part. This means, even though the space-charge effect generally increases the overall transient emittance, the cooling effect caused by the beam self-fields at extraction can still be clearly observed downstream the beam line. It reveals that details of the photoemission can influence the downstream beam quality.

CONCLUSION

The beam self-fields induced cooling effect on the cathode surface is demonstrated through photoemission-model incorporated beam dynamics simulations in high gradient rf injectors. Obtained simulation results have shown a peak to peak variation of about 30% for the intrinsic surface emittance while a reduction of roughly 10% in the mean intrinsic emittance along the exemplary emission curve. Strong nonlinear correlations of the sliced intrinsic emittance with time are observed in the space-charge dominated emission regime. The impact of the photoemission on downstream beam qualities is evidenced by further particle tracking simulations. It can be summarized, that the cooling effect of the beam self-fields on the cathode surface is of significance for understanding the formation of the intrinsic slice emittance of required electron bunches at extraction. This is particularly the case for the bunch extraction near or close to the space-charge dominated emission regime. It should be also noted, that the beam self-fields induced cathode effect(s) should be included in the associated beam dynamics modeling for high gradient RF guns. This is beneficial for more accurately determining the overall emittance budget right after the injector, of which a major part is occupied by the intrinsic emittance.

REFERENCES

[1] W. Decking and H. Weise, "Commissioning of the European XFEL Accelerator", in *Proc. IPAC2017*, Copenhagen, Denmark, May 2017, paper MOXAA1, pp. 1-6.

[2] S. Schreiber and B. Faatz, "The free-electron laser FLASH", *High Power Laser Science and Engineering*, 3, 2015, E20.

[3] F. Stephan and M. Krasilnikov, "High Brightness Photo Injectors for Brilliant Light Sources", in *Chapter of the book "Synchrotron Light Sources and Free-Electron Lasers"*, editors E. Jaeschke, S. Khan, J.R. Schneider, J.B. Hastings, Springer International Publishing Switzerland, ISBN 978-3-319-04507-8, 2016.

[4] M. Krasilnikov, F. Stephan *et al.*, "Experimentally minimized beam emittance from an L-band photoinjector", *Phys. Rev. ST Accel. Beams,* vol. 15, p. 100701, 2012.

[5] Y. Chen *et al.*, "Space-Charge Dominated Photoemission in High Gradient Photocathode RF Guns", in *Proc. LINAC18*, Beijing, China, Sep. 2018, paper THPO116, pp. 941-944.

[6] Y. Chen, M. Krasilnikov *et al.*, "Modeling and simulation of RF photoinjectors for coherent light sources", NIM A 889 pp.129–137, 2018.

[7] Kevin L. Jensen, Barbara L. Jensen *et al.*, Theory of photoemission from cesium antimonide using an alpha-semiconductor model, *Journal of Applied Physics,* 104, p. 044907, 2008.

[8] Kevin L. Jensen, N. A. Moody *et al.*, Photoemission from metals and cesiated surface, *Journal of Applied Physics* 102, p. 074902, 2007.

[9] D. Sertore *et al.*, Optical Properties of Cesium Telluride in *Proc. 8th European Particle Acc. Conf.*, Paris, France, 2002, pp. 1810–1812.

[10] C. Hernandez-Garcia, M. Krasilnikov *et al.*, "Charge production studies from Cs2Te photocathodes in a normal conducting RF gun", *NIM A,* vol. 871, pp. 97–104, 2017.

[11] M. Krasilnikov *et al.*, "Recent Electron Beam Measurements at PITZ with a New Photocathode Laser System", in *Proc. PAC09*, Vancouver, British Columbia, Canada, May 2009, paper MO6RFP057, pp.491-494.

[12] K. Floettmann, "Estimation of the thermal emittance of electrons emitted by cesium telluride photocathodes", in *Proc. FEL97*, Beijing, China, Aug. 1997, DESY-TESLA-FEL-97-06F.